

RESEARCH ARTICLE

Computational Modeling Reveals a Catch-and-Guide Interaction Between Kinesin-1 and Tubulin C-Terminal Tails

Trini Nguyen¹  | Steven P. Gross^{2,3}  | Christopher E. Miles^{1,4} 

¹Center for Complex Biological Systems, University of California, Irvine, Irvine, California, USA | ²Department of Developmental and Cell Biology, University of California, Irvine, Irvine, California, USA | ³Department of Physics, University of California, Irvine, Irvine, California, USA | ⁴Department of Mathematics, University of California, Irvine, Irvine, California, USA

Correspondence: Christopher E. Miles (chris.miles@uci.edu)

Received: 2 July 2024 | **Revised:** 11 February 2025 | **Accepted:** 28 February 2025

Funding: This work was supported by Hellman Foundation; National Science Foundation; National Institutes of Health.

Keywords: computational modeling | cytoskeleton | kinesin | microtubules | tubulin

ABSTRACT

The delivery of intracellular cargoes by kinesins is modulated at scales ranging from the geometry of the microtubule networks down to interactions with individual tubulins and their code. The complexity of the tubulin code and the difficulty in directly observing motor-tubulin interactions have hindered progress in pinpointing the precise mechanisms by which kinesin's function is modulated. As one such example, past experiments show that cleaving tubulin C-terminal tails (CTTs) lowers kinesin-1's processivity and velocity on microtubules, but how these CTTs intertwine with kinesin's processive cycle remains unclear. In this work, we formulate and interrogate several plausible mechanisms by which CTTs contribute to and modulate kinesin motion. Computational modeling bridges the gap between effective transport observations (processivity, velocities) and microscopic mechanisms. Ultimately, we find that a guiding mechanism can best explain the observed differences in processivity and velocity. Altogether, our work adds a new understanding of how the CTTs and their modulation via the tubulin code may steer intracellular traffic in both health and disease.

1 | Introduction

The transport of cargoes along microtubule tracks by kinesin motors is essential to a variety of cellular functions, and impairments are associated with an array of diseases [1]. The complexity and robustness of this transport system are achieved through the intricate regulation of each of its components [2].

One highly and dynamically regulated component is the microtubule tracks [3]. Microtubules are hollow cytoskeletal filaments, consisting of a lattice of α and β tubulin heterodimers, each with a carboxy-terminal tail (CTT) region emanating outward [4]. Microtubules are highly regulable via a zoo of modifications

including those that target CTT directly, such as tyrosination and polyglutamylation. The so-called “tubulin code” hypothesis states that this combinatorial complexity in tubulin heterogeneity facilitates intricate regulation of intracellular traffic [5]. This is supported by observations that tyrosination steers intracellular traffic to peripheries [6, 7] and that a variety of disease states are associated with perturbations to tubulin modifications [8, 9].

Despite convincing evidence that the tubulin code steers intracellular traffic, details of the interactions between motors and CTTs remain less clear. Wang and Sheetz [10] showed that cleaving CTTs with subtilisin lowered the processivity (run lengths before detaching) of both kinesin-1 and dynein. Based

on earlier structural studies showing that the kinesin binding site is not in the CTT region of tubulin [11], the authors conclude that CTT must have an otherwise unspecified “weak attachment” effect. A more recent study also found decreased processivity and a significant decrease in velocity for kinesin-1 walking on CTT-cleaved microtubules [12], shown in Figure 1. This raises the central question of this work: what role do the CTTs play in kinesin movement? One is tempted to speculate, as previous authors do, that a weak tethering with CTTs “catch” otherwise detaching motors. However, this fails to clearly explain the decreased velocity from their severing. Alternatively, if CTTs facilitate any portion of the processive stepping cycle, this does not obviously affect run lengths. Although atomistic-scale simulations have extensively investigated interactions of CTTs with motors [13–17] questions of this timescale are challenging to address.

In this work, we develop coarse-grained biophysical computational models to explore and vet possible models of the contribution CTTs provide to kinesin-1’s processive movement. The modeling scale is chosen to leverage the immense detail known of the chemomechanical stepping cycle of kinesin-1 [18, 19]. We ask what plausible interactions with this cycle can quantitatively explain the results of [12] with CTTs lengthening motor processivity and speeding up velocity in a reasonable parameter regime. We investigate three conceptual models shown in Figure 1: (1) CTTs catch motors that unbind from the microtubule, (2) they guide the motor head’s diffusive search for the next microtubule-binding site during stepping, and (3) they stimulate ADP release similarly to microtubule-stimulated ADP release [20]. Each of these models has some mechanistic basis and plausibility in explaining the results. To evaluate each model, we translate each

into a computational counterpart and compare them with the data of [12]. After validation, we find that the “catch” model does not explain both processivity and velocity experimental data simultaneously. We also find that the ADP-release model does not reconcile processivity on cleaved microtubules with reasonable parameters. However, a “catch-and-guide” model, where CTTs both facilitate the search for a new binding site and catch unbinding motors, can explain all available observed data.

2 | Results

2.1 | By Catching Unbound Motors, CTTs Can Extend Their Run Lengths on the Microtubule, but Would Also Slow Them Down in the Process

We simulate a motor (not bound to any cargo) walking on the microtubule using a Gillespie algorithm [21]. The simulation is based on a model of the kinesin-1 step-cycle in existing literature [22] and describes the key ADP, ATP, and phosphate release reactions that shape the process. This general model of kinesin stepping, shown schematically in Figure 2, is as follows: one of the motor’s heads strongly binds to the microtubule when it comes into contact with the microtubule and ADP is released from that head. ATP then binds to this head, which results in a change of orientation in which the other head now switches forward. This head now needs to come into contact with the next binding site on the microtubule and await ADP release to finish the motor’s step. If phosphate release on the bound head happens before ADP is released from the front dangling head, then the motor becomes unbound. This model does not consider interactions between a CTT and the motor. To consider

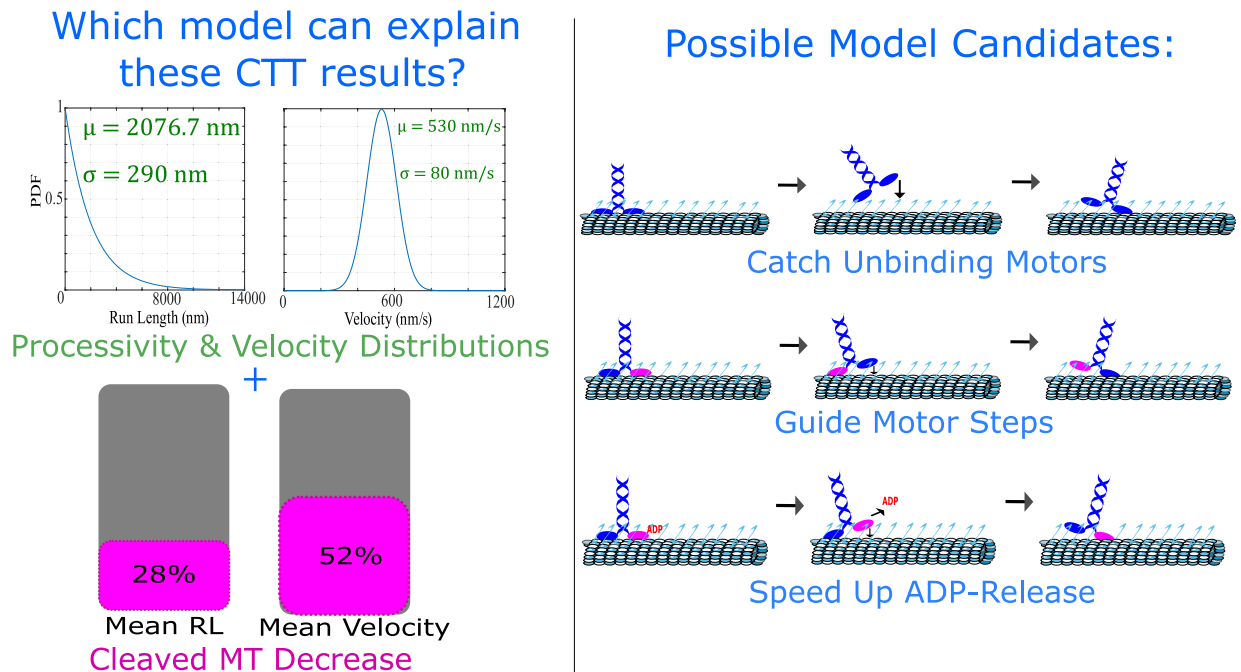


FIGURE 1 | Possible CTT mechanisms for motor processivity assistance. Left: The ideal model that can explain how CTTs can assist motors on microtubules will need to explain all of the displayed data, with physiologically feasible parameters. Right: Possible models explored that may explain the data. First model: CTTs catch motors as they unbind from the microtubule and pull them back. Second model: One of the motor’s heads is dangling as it searches for a microtubule-binding site to take the next step. CTTs help guide this dangling head to that next binding site. Third model: CTTs speed up ADP release.

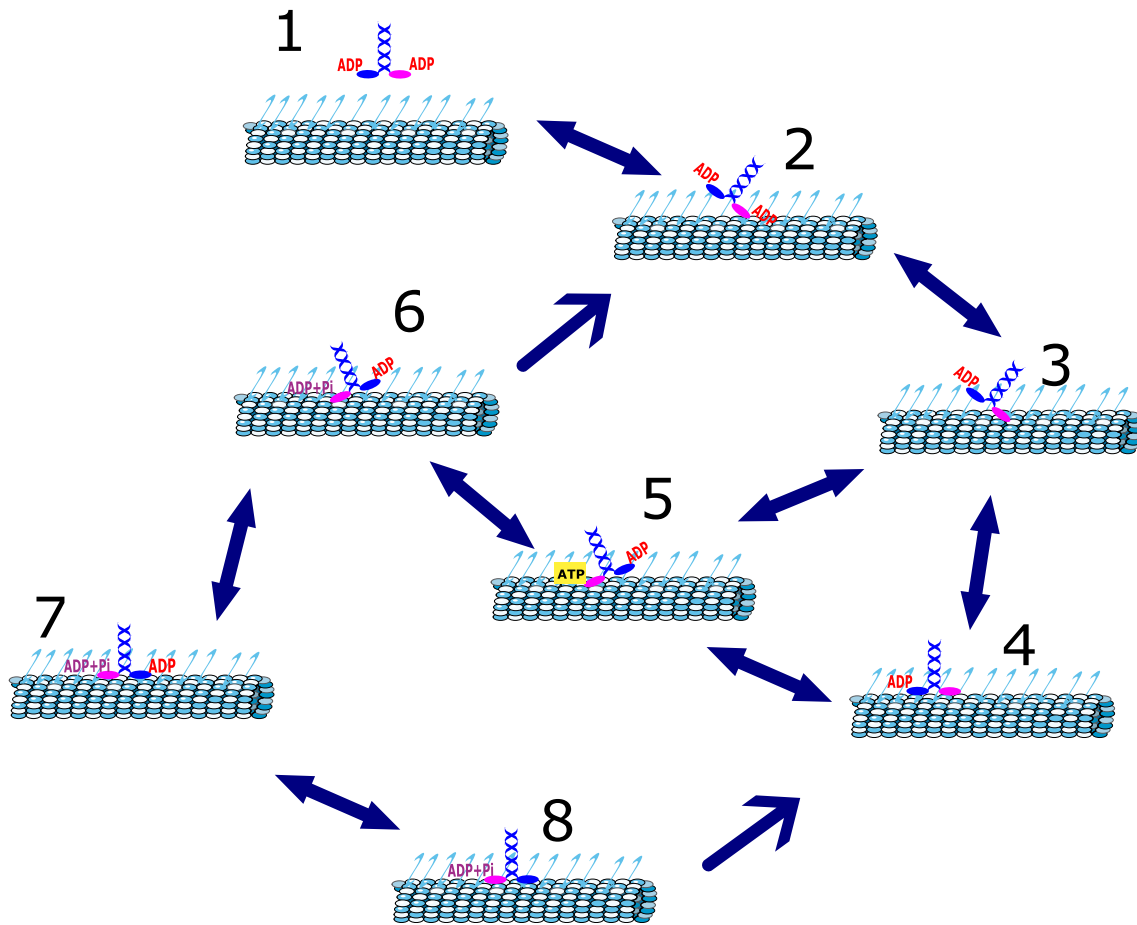


FIGURE 2 | Model of kinesin stepping in existing literature. Current models of stepping do not consider the motor's interaction with the CTT. The motor can strongly bind to the microtubule when ADP is released from the microtubule-bound head (State 3) [22]. ATP binding to this head results in the trailing head (blue head) switching forward (State 5). ADP release from this head results in another strong binding to the microtubule (State 8), which allows the motor to finish taking one step.

CTTs assisting the motor, we included another state (State 9 in Figure 3a) in this model, where a CTT can catch the motor as it unbinds from the microtubule and hold it until it can rebind to the microtubule. The model is not exhaustive in the possible nucleotide states of both heads, nor does it consider backstepping [23], but is chosen as a minimal model with past success [22] in capturing the key features of kinesin-1's movement. Most of the parameters were taken from estimates in the existing literature (Table 1). The remaining three unknown parameters of this model are then fitted to the experimental data from [12], which included distributions of run length and velocity of motors on wildtype microtubules and fold comparisons of mean run length and velocity of motors on microtubules with CTTs cleaved compared to motors on wildtype microtubules. With the addition of the "caught state" State 9, we hoped that this catching mechanism would allow the motor to walk on the microtubule further than when CTTs are absent, as seen in [12]. Indeed, we were able to fit this model to the experimental processivity results (Figure 3b), and there does seem to be a processivity advantage that CTTs provide to motors (Figure 3c). The resulting parameter fits can be found in Table 1. Notably, parameter fits for steps that are not rate-limiting produce unfeasibly large values, but these steps do not shape the macroscopic observed quantities. Thus, by catching motors, CTTs can decrease unbinding events, and the motors can stay on the microtubules longer, resulting

in longer run lengths. However, the model's velocity is unable to match that of the experimental data (Figure 3d), since there is an additional state in the model that does not provide any method for faster runs. When the motor is attached to the MT via CTT-only, there is no stepping, so the more times the CTTs "catch" the motor and increase its processivity, the slower the average velocity is (Figure 3d). In sum, a model where CTTs help motors by only catching them before unbinding from microtubules seems to fail to explain the observations.

2.2 | Guiding Dangling Motor Heads Close to the Next Microtubule Binding Site Results in an Increase in Both Run Length and Velocity

Since the catching mechanism does produce higher processivity, we opted to retain it in the next model explored. In pursuit of a model that includes a speed-up in velocity, we predicted that CTTs may interact with the motor earlier in the kinesin step-cycle while the motor is still bound to the microtubule. Specifically, when one motor head is bound to the microtubule, the other is unbound and searching for the next binding site to take its next step. In this unbound position, the motor may bind to a nearby CTT, and since CTTs are very near microtubule-binding sites [5], the CTT could speed up this dangling head's

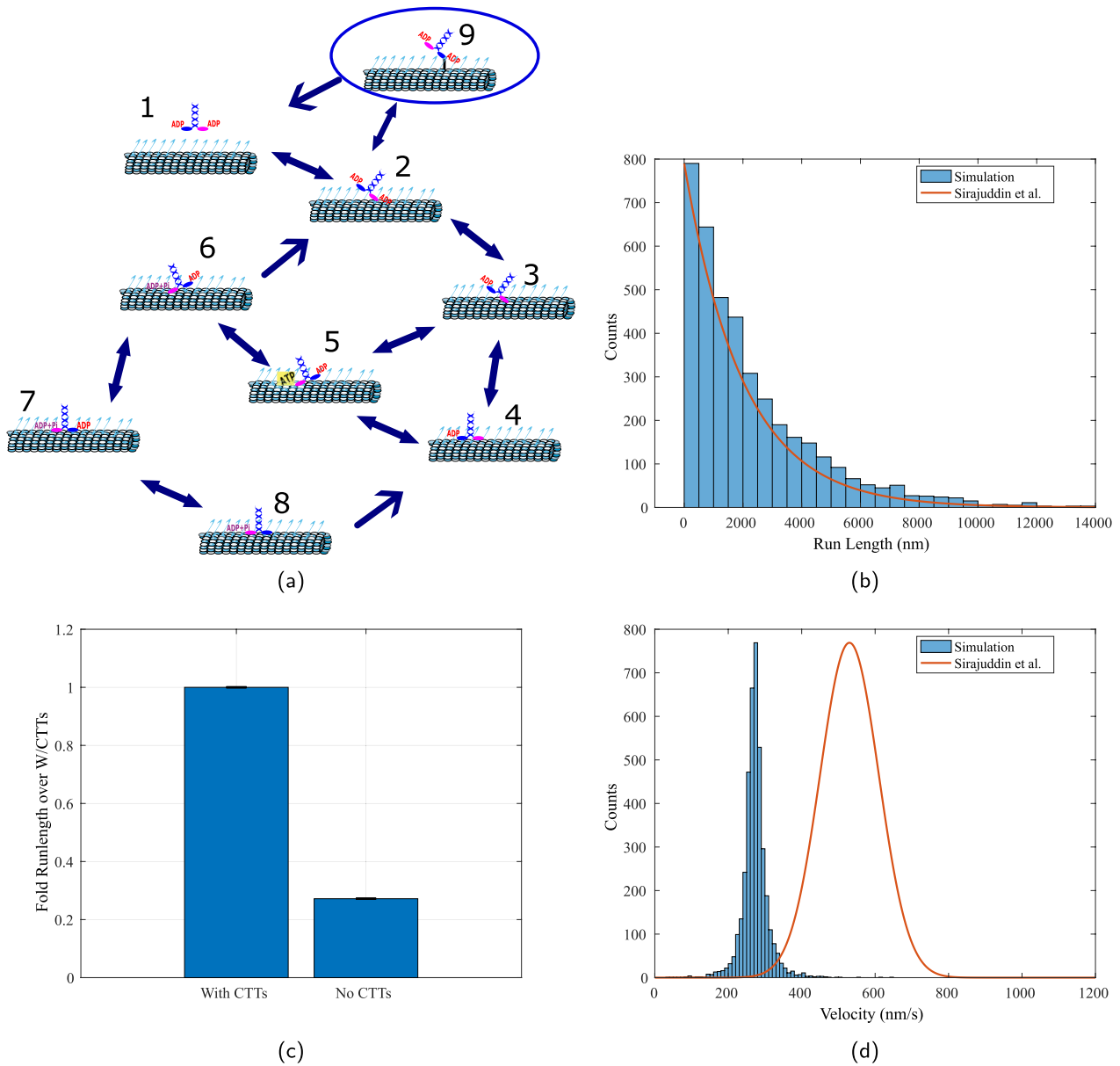


FIGURE 3 | Catching motors results in longer run lengths but slower velocities. (a) This model is similar to Figure 2, with an additional state (State 9) that considers the CTT catching unbound motors. The model can recapture observed run lengths (Anderson-Darling test, $p = 0.0732$) in (b) but fails to do so for velocity (Anderson-Darling, $p \ll 0.05$) in (d) $n = 4000$ simulations using parameters from Table 1. Red curves are wildtype (with CTTs) data from [12]. (c) Mean run lengths for the model in (a) (with CTTs) taken from 4000 simulations. Mean run lengths from the model in Figure 2 (with CTTs cleaved from the microtubule) were then compared to these means. $n = 3 \pm \text{SEM}$.

diffusive search for the next binding site by guiding this head to that site. Figure 4a shows the different states of this model, where a CTT binds to the dangling motor head in State 9 and guides it to the microtubule in State 7. A speed-up in velocity would require the transitions from State 6 to 9, then 7 to be overall faster than the transitions from 6 to 7. The catching mechanism from Figure 3 is now in State 10, where if the bound head becomes unbound, the CTT still holds on to the motor. However, this model does not need to solely depend on State 10 to extend run lengths, as the addition of State 9 allows for another possible state the motor can enter from State 6 that is not back to State 2 (and subsequently, detachment to State 1).

To explore the catch and guide model's ability to explain the experimental run length and velocity trends, we repeat the fitting

procedure, allowing all previously fitted and newly introduced parameters to vary freely, resulting in 4 total. With the addition of the guiding mechanism, we now see the Catch+Guide model can match both the experimental data's run length and velocity distributions (Figure 4b,c). In addition, the fold differences in run length and velocity between setups with CTTs and those with cleaved CTTs also match those that were previously observed [12] (Figure 4d,e). The resulting parameter fits can be found in Table 1 and show that a subset of fitted parameters change dramatically from the catching model, most notably the microtubule-binding rate.

It is not surprising that a more complex model should be able to fit more data. However, we argue this model is the minimal complexity necessary to explain both run lengths and

TABLE 1 | Parameters used in simulations.

Parameter (s^{-1})	Catch	Catch and guide	Stimulated ADP-release	States, citation
Motor-MT on-rate	1.8e4	410	3973	1 to 2, 3 to 4, 6 to 7, fitted
Motor-MT off-rate	0.7	0.7	0.7	2 to 1, 4 to 3, 7 to 6 [24–27]
Motor-CTT on-rate	2.6e6	767	437	2 to 9 in Catch, 6 to 9 in Catch+Guide and ADP, 11 to 10 in ADP, fitted
Motor-CTT off-rate	548	76	370	9 to 1 in Catch, 9 to 6 and 10 to 1 in Catch+Guide, 9 to 6 and 10 to 11 in ADP, fitted
Motor-MT CTT-assisted on-rate	—	510	—	9 to 7 in Catch+Guide, fitted
Loaded ADP off-rate	120	120	120 for WT; 50 for cleaved	7 to 8, 9 to 10 in ADP, fitted for ADP [28, 29]
Unloaded ADP off-rate	2	2	2 for WT; 0.8 for cleaved	2 to 3, fitted for ADP [28, 29]
Phosphate on-rate	0.001	0.001	0.001	6 to 5 [30]
Phosphate off-rate	100	100	100	6 to 2 [31]
ADP on-rate	4000	4000	4000	3 to 2, 8 to 7, 10 to 9 in ADP [31]
ATP on-rate	100	100	100	3 to 5, 4 to 5 [31]
ATP hydrolysis rate	200	200	200	5 to 6 [31]

Abbreviations: MT: microtubule, WT: wildtype.

velocity trends. From Figure 4f, we see that this model indeed does not enter State 10 often and thus does not rely on it to fit observed run lengths. We also considered a model that includes only the guiding mechanism without any catching assistance (Figure S1), and this model's predictive power in predicting processivity from only velocity was comparable to the Catch+Guide model, with no significant difference in the predictive errors. From this, we conclude that the catch and guide portions of the model have distinct, but equally important influences. To understand and validate this model at a finer scale, we conducted a Brownian dynamics simulation of a dangling motor head performing a diffusive search for the next microtubule-binding site, with results shown in (Figure S3a). These simulations show that CTTs can decrease the space that the motor head must diffusively explore to bind and thus decrease its search time by about 50% (Figure S3b). While the microsecond timescale of these diffusive searches is much faster than the millisecond stepping cycle that is rate-limited by chemical events, the relative reduction in search time with CTTs provides important mechanistic insight. Previous modeling work incorporating neck linker mechanics and tethered diffusion [32] demonstrated that the accessibility of binding zones during diffusive searches strongly influences stepping outcomes. In this context, our finding that CTTs cut diffusion times in half suggests they bias the rapid diffusive component of each step toward the forward binding site, helping explain the increased backstepping observed when CTTs are removed [33]. The agreement in both microscopic and macroscopic trends suggests that CTTs acting as a guide for dangling motor heads to the next microtubule-binding site is a compelling and plausible mechanism.

2.3 | The Model That Considers CTTs Stimulating ADP Release Cannot Explain Experimental Data With Reasonable Parameters

Previous studies have found that when both kinesin motor heads bind to the microtubule, the tubulin from the microtubule stimulates ADP release at a faster rate of $\sim 120 s^{-1}$ [28, 29]. Since CTTs are largely comprised of tubulin, we speculated whether the CTT could also stimulate ADP release from the motor heads. To explore the possibility of this mechanism, we allowed in our simulations for ADP release to occur at a stimulated rate if the motor binds to the CTT, as well as when it binds to the microtubule (Figure 5a). Since the previously estimated release rate of $\sim 120 s^{-1}$ was obtained from experiments using wild-type microtubules (with CTTs), the release rate for microtubules with cleaved CTTs may be slower to result in slower motor velocities. Thus, to evaluate the predictive power of this model, we first fitted the unknown motor-microtubule-binding rate, motor-CTT binding rate, and motor-CTT unbinding rate to the wild-type processivity and velocity data, using a fixed stimulated ADP-release rate of $\sim 120 s^{-1}$. We then fitted the unknown slower stimulated ADP-release rate for cleaved microtubules to the cleaved microtubule experimental velocity data, with fixed values for the motor-microtubule and -CTT binding and motor-CTT unbinding rates, obtained from the previous fit with the wild-type data. To obtain reasonable fits with the experimental velocity, this slowed-down rate had to be decreased by about 50% (Table 1). With these fitted values, we predicted the cleaved microtubule experimental processivity data (Figure 5b). This prediction resulted in no decrease in run length, which does not match the experimental data. We

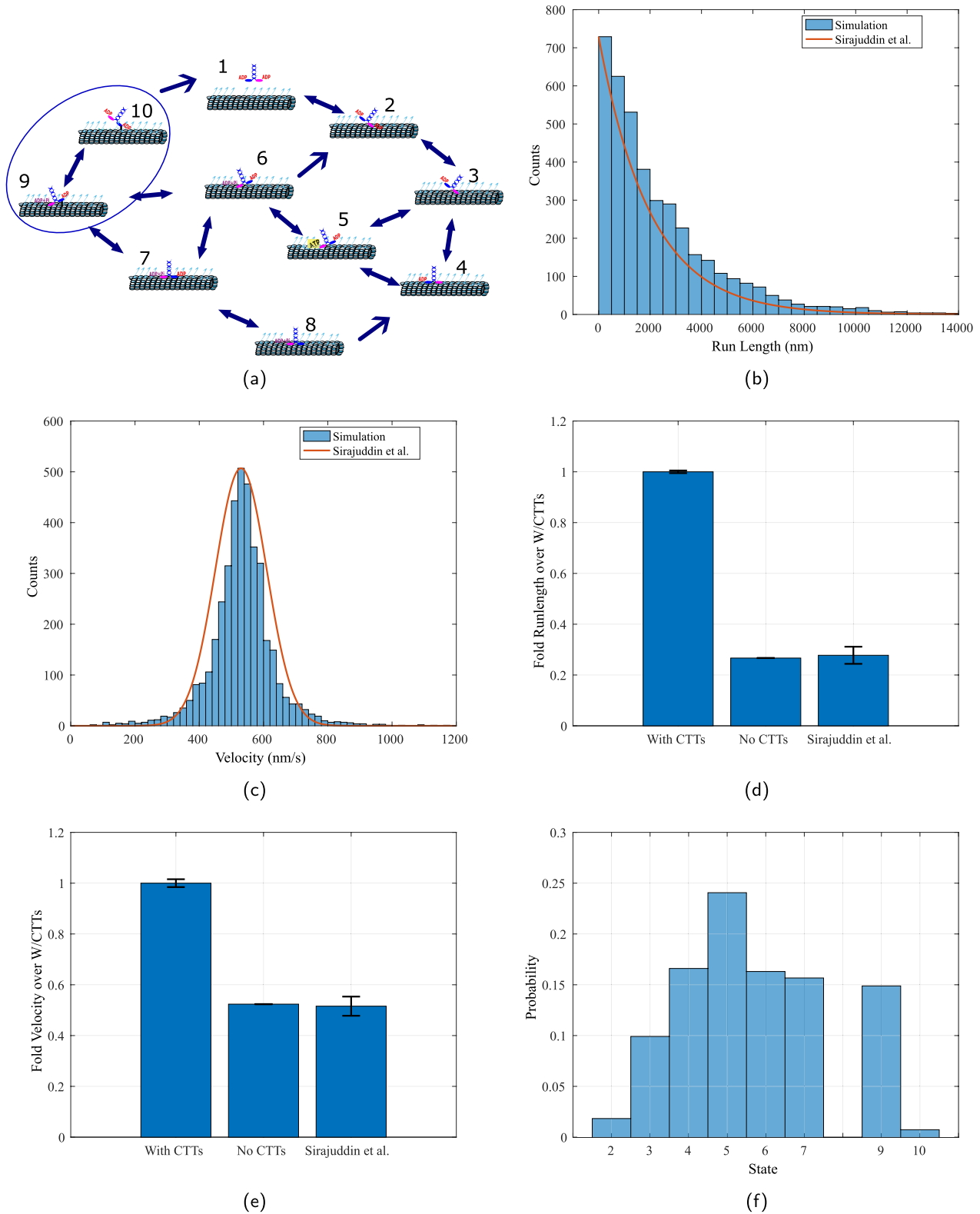


FIGURE 4 | Legend on next page.

then tried to slow down the unloaded (one-headed) stimulated ADP-release rate that occurs from States 2 to 1 in the cleaved microtubule simulations as well. Since the fitted loaded rate decreased by about 50%, we lowered the unloaded rate to the same magnitude. By doing so, we retained the match in

velocity, so the loaded rate does not affect velocity. We also observed a reduction in processivity; however, the reduction was not enough to match the experimental data. Thus, it is not likely that CTTs can assist motors solely by stimulating ADP release.

3 | Discussion

Previous experiments have demonstrated that tubulin CTTs increase kinesin-1's processivity and velocity. We use computational modeling to ascribe novel mechanistic understanding to these observations. By quantitatively vetting conceptually plausible models, the emergent model is a "guiding" one where CTTs provide a weak tethering that facilitates the motor head's search for the next binding site. Beyond direct agreement with the past data, our emergent model is also in conceptual agreement with other observations. Without CTTs facilitating the search to the next forward binding site, backstepping is favored [33], although we have not explicitly incorporated backstepping in the model here due to the lack of opposing force on the motor [23]. Moreover, this guiding effect should have no effect on cargo-MT distance, in agreement with observations in [34]. In [12], the authors also report that restoring β -tubulin CTT recovers kinesin-1 velocity. A previous biophysical modeling approach [35] speculated that negatively charged CTTs interact with positively charged kinesin neck linkers. However, the recovery of velocity with β -tails seems in closer agreement to our guiding model, as β -tubulin tails are adjacent to bound heads, whereas α -tubulin tails are in proximity with the neck linker [36]. Our Brownian dynamics simulations quantitatively support this guiding mechanism—CTTs reduce the diffusive search time from 5×10^{-7} s to 2.5×10^{-7} s (Figure S3b). While these absolute timescales are much faster than the overall stepping cycle, the relative differences in binding zone accessibility during diffusive searches can significantly influence the probability of successful forward stepping versus detachment or backstepping, similar to how neck linker mechanics were shown to regulate motor properties through tethered diffusion [32]. Moreover, the guiding mechanism is found speculatively in other past work [37, 38]. The guiding model has direct ramifications for achieving a more mechanistic understanding of the tubulin code: post-translational modifications such as polyglutamylation that increase the length of the CTTs could easily alter how they bind to the searching motor head, and other PTMs that increase or decrease the affinity of the CTT for the kinesin would then directly alter the CTTs effects on kinesin processivity and velocity.

Among many limitations of our study, we acknowledge that using a coarse-grained description of the kinesin-1 stepping cycle necessarily omits additional possible states for each motor head and transitions between them. For instance, we do not explicitly include aspects like ATP binding to both heads simultaneously [19], backstepping pathways [33], or intermediate nucleotide states [22]. Other computational studies [39] have investigated variations of models similar to the one considered here with

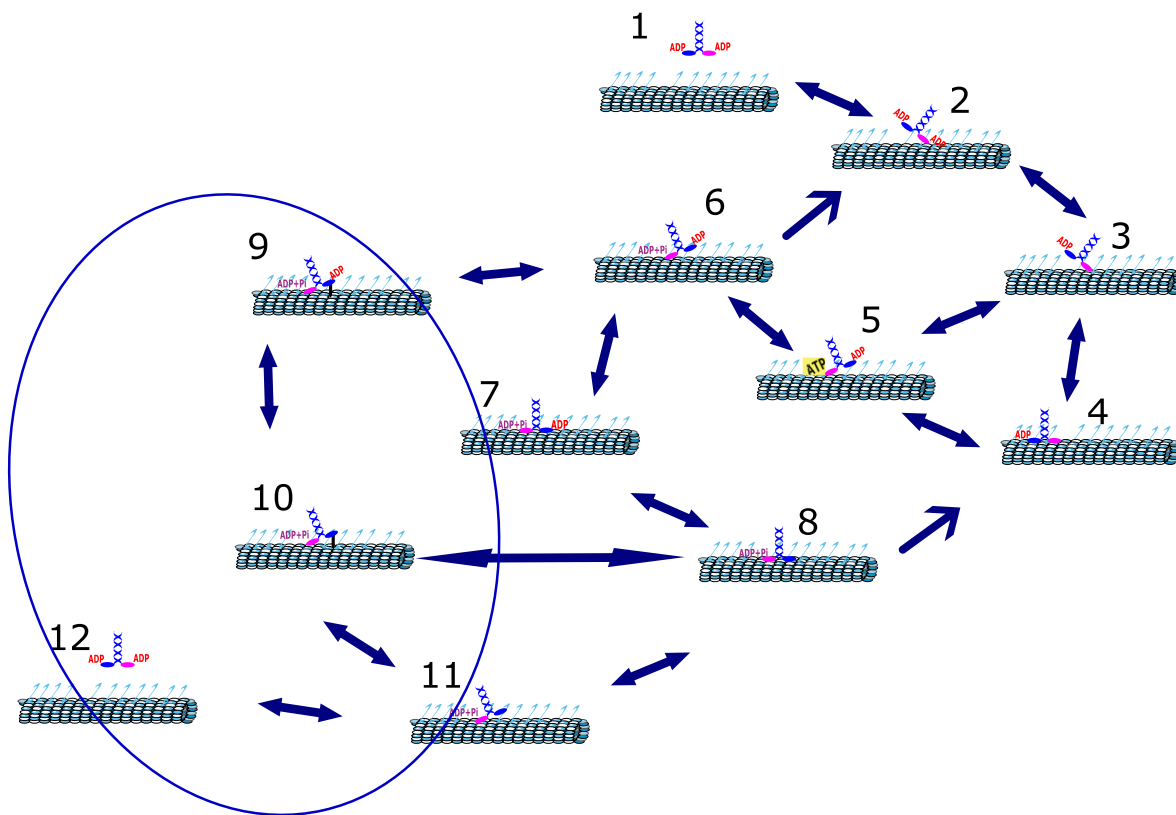
additional pathways involving phosphate release timing that could potentially explain some CTT effects through ADP release modulation. While such expanded models are possible in our framework and worth future investigation, all extensions introduce additional parameter complexity that seems unresolvable given the resolution of available experimental data. This is particularly challenging in a context where many rate constants must be inferred indirectly from ensemble measurements rather than direct observation of individual transitions. Consequently, we believe our choice represents a pragmatic balance between explanatory complexity and model interpretability. However, because of this simplicity, we cannot rule out that more complex models incorporating additional transitions might provide alternative explanations for CTT's effects on motor function. This highlights an important tradeoff in mechanistic modeling between explanatory completeness and parameter parsimony.

It is important to note that we believe our model applies specifically to kinesin-1, in which this kinesin's positively charged areas on its motor domains have a weak attraction to the negatively charged CTTs [36, 40]. CTT and post-translational modifications are known to affect kinesin-2 [12], kinesin-3 [38], and dynein [13]. However, the investigation of these effects will require the construction of new computational models that reflect the specific mechanochemistry of the motors. We believe that our work provides a template for these future studies.

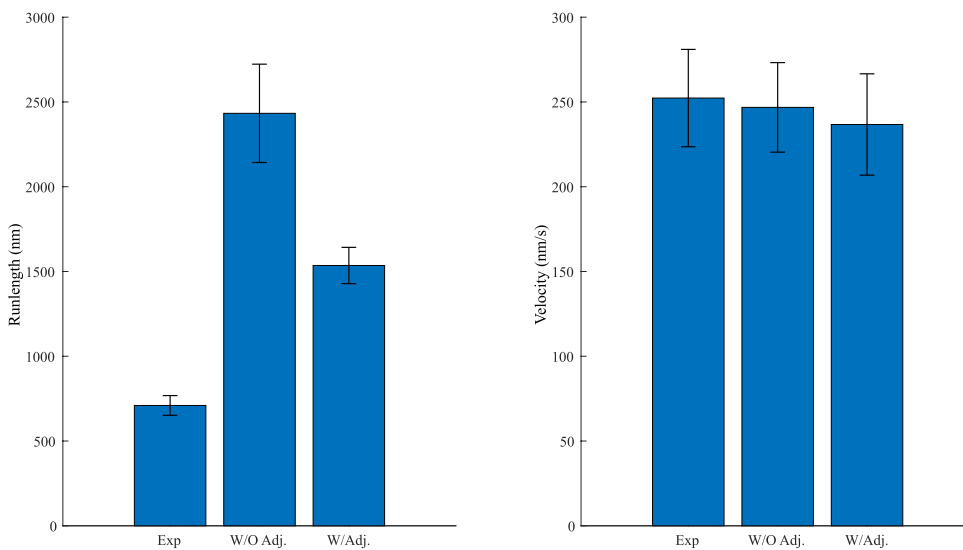
There are several avenues of future interest. Our work investigates the behavior of a single motor, but cargoes are driven by teams. Force production is noted to be changed with the cleaving of CTT [41], likely due to the increase in backstepping [33]. Moreover, kinesins are observed to have a lower affinity for CTT-cleaved microtubules [42], suggesting that binding is also affected. To understand how *in vivo* CTT mediates intracellular traffic, more detailed biophysical models of multi-motor transport [43] and binding [44] must be adapted to incorporate the guiding CTT mechanism. These would be the first steps toward understanding the feedback between the tubulin code and motor transport, including how motors may modulate the code [45] and other mechanical feedbacks [46].

We also believe that our guiding mechanism may be validated directly through imaging advances. For example, perhaps by measuring the movement of the unbound leading motor head of motors on wild-type microtubules vs. cleaved microtubules via light-scattering methods [47]. In this experiment, a result of the motor head's position concentrated in a specific area on wildtype microtubules, and the motor head's position scattered on cleaved microtubules would support our model directly.

FIGURE 4 | CTTs guiding dangling motor heads to the next microtubule-binding site model matches both experimental run lengths and velocities. (a) A CTT binds to the unbound motor head while the other motor head is bound to the microtubule (State 9). The CTT can then guide it to the next microtubule-binding site, ideally speeding up its search for this site. The catching mechanism is still considered in this model (State 10). (b and c) Experimentally observed run lengths (red curve, b) and velocities (c) from [12] are shown against computationally simulated run lengths and velocities (blue bars) from motors on wild-type microtubules (with CTTs). $n = 4000$ simulations. Computational and experimental distributions agree for both run lengths and velocities (Anderson-Darling test, $p = 0.0654, 0.0785$ respectively.) (d and e) Run lengths and velocities presented as ratios over that of the setup with CTTs, as mean \pm SEM, $n = 3$ runs of 4000 simulations each. The final bar shows the ratios of motors on cleaved microtubules data over motors on wild-type microtubules from [12]. (f) Probability of a motor being in a certain state in the model at a given time. States 8 and 4 are the same and thus grouped under State 4.



(a)



(b)

FIGURE 5 | CTTs stimulating ADP release model cannot explain data with reasonable parameters. (a) Diagram of the model. (b) Fitted model results do poorly match experimental data, even when the unloaded ADP-release rate from State 2 was adjusted.

4 | Methods

4.1 | Kinesin Step Cycle Simulation

We simulate an unbound kinesin-1 motor diffusing to a microtubule, binding to it, and walking on it. Transitions between

each state are modeled as Poisson processes, with rates from Table 1. These transitions are simulated using a Gillespie algorithm [21]. At each time step, the time to the next step is computed as

$$\Delta t = \frac{1}{\sum r_i} \cdot \ln \frac{1}{w_1}$$

where r is the rate of the i th reaction and w_1 is a random number between 0 and 1. To determine which reaction will occur at $t + \Delta t$, we find the smallest integer i that satisfies

$$\sum_{i=1}^i r'_i > w_2 \sum_i r_i$$

where w_2 is another random number between 0 and 1. We take run length to be the entire length the motor walks on the microtubule until it falls off completely from the microtubule (the motor unbinds from the microtubule and a CTT). We take velocity to be this run length over the total time the motor was on the microtubule. The simulation is written in Matlab.

4.1.1 | Motor Head Diffusive Search Simulation

To further investigate the Catch+Guide model, we conducted a Brownian Dynamics simulation of the dangling motor head searching for the next microtubule-binding site (Figure S3a). The searching head is modeled as a sphere with radius $r=3$ nm, tethered by the neck linker which is modeled as a worm-like chain, similar to other models of the neck linker [32]. The force that this neck linker exerts on the motor head is expressed as

$$f = \frac{k_B T}{L_p} \left(\frac{1}{4} \left(1 - \frac{d}{L_c} \right)^2 - \frac{1}{4} + \frac{d}{L_c} \right)$$

where $k_B T$ is the Boltzmann constant, L_p is the persistence length of the neck linker (0.7 nm), d is the end-to-end distance of the neck linker, and L_c is the contour length (0.364 nm per amino acid, 14 residues total). The position of the searching head $X(t)$ can then be expressed as the stochastic differential equation

$$dX(t) = \frac{1}{\epsilon} f(X(t)) dt + \sqrt{2D} dB(t)$$

where $\epsilon = 6\pi\eta r$ is the drag coefficient, η is the viscosity (taken to be that of water), $D = k_B T / \epsilon$ is the motor head diffusion coefficient, and $B(t)$ is Brownian motion. This equation is numerically solved using the Euler-Maruyama method. At every timestep, new random vectors from a uniform distribution between 0 and 1 are chosen until a vector is chosen such that the motor head does not overlap with the microtubule. The motor head can bind to either the CTT or microtubule-binding site if it is within 1 nm from either target. Both the CTT and microtubule-binding site are positioned 8 nm away from where the searching motor head is tethered, and the CTT is 8-nm long. If the motor head binds to the CTT, it continues its diffusive search but is now restricted by the CTT's reach.

4.2 | Model Fitting

To infer the parameters of our models, we fit all models to experimental data from [12] using a simple approximate Bayesian computation algorithm [48] and selecting the parameters that resulted in the smallest absolute error (maximum a posteriori

estimate). Uniform priors were used. The available data consist of processivity mean and variance, velocity mean and variance, and fold comparisons of the cleaved microtubule cases for both processivity and velocity means. The cross-validation analysis (Figure S1) was performed similarly, but only using the velocity data for training and subsequently the processivity data for testing. The simple approximate Bayesian computation algorithm is as follows:

while $n \leq N$ **do**

 Sample θ^* from prior $\pi(\theta)$

for $i = 1$ to N **do**

 Determine predicted run lengths and velocities using θ^*

end for

 Calculate mean and variance of predicted run lengths and velocities

 Calculate absolute error between predicted and experimental values

end while

 Take θ^* that resulted in the smallest error.

To produce Figure S2, the above algorithm was used on the ADP-release model, and the parameters that resulted in the lowest 1% absolute error were chosen. Only experimental data from the wild-type microtubules were used.

Acknowledgments

C.E.M. and T.N. were partially supported by a University of California Society of Hellman Fellows fund. S.P.G. was partially supported by NIH R01 GM123068. C.E.M. was partially supported by NSF CAREER DMS 2339241.

Ethics Statement

The authors have nothing to report.

Conflicts of Interest

The authors declare no conflicts of interest.

Data Availability Statement

MATLAB code to reproduce our results (compatible with version R2020a) is available at <https://github.com/trininguyen/CTTassist>.

Peer Review

The peer review history for this article is available at <https://www.webofscience.com/api/gateway/wos/peer-review/10.1111/tra.70002>.

References

1. K. J. De Vos, A. J. Grierson, S. Ackerley, and C. C. J. Miller, "Role of Axonal Transport in Neurodegenerative Diseases," *Annual Review of Neuroscience* 31 (2008): 151–173, <https://doi.org/10.1146/annurev.neuro.31.061307.090711>.
2. K. J. Verhey and J. W. Hammond, "Traffic Control: Regulation of Kinesin Motors," *Nature Reviews Molecular Cell Biology* 10, no. 11 (2009): 765–777, <https://doi.org/10.1038/nrm2782>.

3. L. Balabanian, A. R. Chaudhary, and A. G. Hendricks, "Traffic Control Inside the Cell: Microtubule-Based Regulation of Cargo Transport," *Biochemist* 40, no. 2 (2018): 14–17, <https://doi.org/10.1042/BIO04002014>.
4. E. Nogales, S. Wolf, and K. Downing, "Structure of the Alpha beta Tubulin Dimer by electron Crystallography," *Nature* 391, no. 6663 (1998): 199–203, <https://doi.org/10.1038/34465>.
5. C. Janke and M. Magiera, "The Tubulin Code and Its Role in Controlling Microtubule Properties and Functions," *Nature Reviews. Molecular Cell Biology* 21, no. 6 (2020): 307–326, <https://doi.org/10.1038/s41580-020-0214-3>.
6. Y. Konishi and M. Setou, "Tubulin Tyrosination Navigates the Kinesin-1 Motor Domain to Axons," *Nature Neuroscience* 12 (2009): 559–567, <https://doi.org/10.1038/nn.2314>.
7. J. W. Hammond, C. F. Huang, S. Kaeck, C. Jacobson, G. Banker, and K. J. Verhey, "Posttranslational Modifications of Tubulin and the Polarized Transport of Kinesin-1 in Neurons," *Molecular Biology of the Cell* 21, no. 4 (2009): 572–583, <https://doi.org/10.1091/mbc.e09-01-0044>.
8. E. D. McKenna, S. L. Sarbanes, S. W. Cummings, and A. Roll-Mecak, "The Tubulin Code, From Molecules to Health and Disease," *Annual Review of Cell and Developmental Biology* 39 (2023): 331–361, <https://doi.org/10.1146/annurev-cellbio-030123-032748>.
9. O. Wattanathamsan and P. Varisa, "Post-Translational Modifications of Tubulin: Their Role in Cancers and the Regulation of Signaling Molecules," *Cancer Gene Therapy* 30, no. 4 (2023): 521–528, <https://doi.org/10.1038/s41417-021-00396-4>.
10. Z. Wang and M. P. Sheetz, "The C-Terminus of Tubulin Increases Cytoplasmic Dynein and Kinesin Processivity," *Biophysical Journal* 78, no. 4 (2000): 1955–1964, [https://doi.org/10.1016/S0006-3495\(00\)76743-9](https://doi.org/10.1016/S0006-3495(00)76743-9).
11. P. K. Marya, Z. Syed, P. E. Fraylich, and P. A. M. Eagles, "Kinesin and Tau Bind to Distinct Sites on Microtubules," *Journal of Cell Science* 107, no. 1 (1994): 339–344, <https://doi.org/10.1242/jcs.107.1.339>.
12. M. Sirajuddin, L. Rice, and R. Vale, "Regulation of Microtubule Motors by Tubulin Isoforms and Post-Translational Modifications," *Nature Cell Biology* 16, no. 4 (2014): 335–344, <https://doi.org/10.1038/ncb2920>.
13. N. Tajjelyato, L. Li, Y. Peng, J. Alper, and E. Alexov, "E-Hooks Provide Guidance and a Soft Landing for the Microtubule Binding Domain of Dynein," *Scientific Reports* 8 (2018): 13266, <https://doi.org/10.1038/s41598-018-31480-9>.
14. Y. Mizuhara and M. Takano, "Biased Brownian Motion of KIF1A and the Role of tubulin's C-Terminal Tail Studied by Molecular Dynamics Simulation," *International Journal of Molecular Sciences* 22, no. 4 (2021): 1547, <https://doi.org/10.3390/ijms22041547>.
15. X.-X. Shi, Y.-B. Fu, S.-K. Guo, P.-Y. Wang, H. Chen, and P. Xie, "Investigating Role of Conformational Changes of Microtubule in Regulating Its Binding Affinity to Kinesin by All-Atom Molecular Dynamics Simulation," *Proteins* 86, no. 11 (2018): 1127–1139, <https://doi.org/10.1002/prot.25592>.
16. A. Pan, A. Pan, B. R. Brooks, and X. Wu, "Molecular Simulation Study on the Walking Mechanism of Kinesin Dimers on Microtubules," *Current Advances in Chemistry and Biochemistry* 1 (2021): 49–64, <https://doi.org/10.9734/bpi/cacb/v1/6918d>.
17. Y.-Z. Geng, L.-A. Lu, N. Jia, B.-B. Zhang, and Q. Ji, "Kinesin-Microtubule Interaction Reveals the Mechanism of Kinesin-1 for Discriminating the Binding Site on Microtubule," *Chinese Physics B* 32, no. 10 (2023): 108701, <https://doi.org/10.1088/1674-1056/acdfc1>.
18. A. Yildiz, M. Tomishige, R. Vale, and P. Selvin, "Kinesin Walks Hand-Over-Hand," *Science (New York, N.Y.)* 303, no. 5658 (2004): 676–678, <https://doi.org/10.1126/science.1093753>.
19. S. M. Block, "Kinesin Motor Mechanics: Binding, Stepping, Tracking, Gating, and Limping," *Biophysical Journal* 92 (2007): 2986–2995, <https://doi.org/10.1529/biophysj.106.100677>.
20. H. Sosa, E. J. G. Peterman, W. E. Moerner, and L. S. B. Goldstein, "ADP-Induced Rocking of the Kinesin Motor Domain Revealed by Single-Molecule Fluorescence Polarization Microscopy," *Nature Structural Biology* 8, no. 6 (2001): 540–544, <https://doi.org/10.1038/88611>.
21. D. T. Gillespie, "Stochastic Simulation of Chemical Kinetics," *Annual Review of Physical Chemistry* 58 (2007): 35–55, <https://doi.org/10.1146/annurev.physchem.58.032806.104637>.
22. K. J. Mickolajczyk, N. C. Deffenbaugh, J. Ortega Arroyo, and W. O. Hancock, "Kinetics of Nucleotide-Dependent Structural Transitions in the Kinesin-1 Hydrolysis Cycle," *Proceedings of the National Academy of Sciences of the United States of America* 112, no. 52 (2015): E7186–E7193, <https://doi.org/10.1073/pnas.1517638112>.
23. B. E. Clancy, W. M. Behnke-Parks, J. O. L. Andreasson, S. S. Rosenfeld, and S. M. Block, "A Universal Pathway for Kinesin Stepping," *Nature Structural & Molecular Biology* 18, no. 9 (2011): 1020–1027, <https://doi.org/10.1038/nsmb.2104>.
24. S. M. Block, L. S. B. Goldstein, and B. J. Schnapp, "Bead Movement by Single Kinesin Molecules Studied With Optical Tweezers," *Nature* 348 (1990): 348–352, <https://doi.org/10.1038/348348a0>.
25. M. Vershinin, B. C. Carter, D. S. Razafsky, S. J. King, and S. P. Gross, "Multiple-Motor Based Transport and Its Regulation by Tau," *Proceedings of the National Academy of Sciences* 104 (2007): 87–92, <https://doi.org/10.1073/pnas.0607919104>.
26. J. Xu, Z. Shu, S. J. King, and S. P. Gross, "Tuning Multiple Motor Travel via Single Motor Velocity," *Traffic* 13, no. 9 (2012): 1198–1205, <https://doi.org/10.1111/j.1600-0854.2012.01385.x>.
27. Q. Li, S. J. King, A. Gopinathan, and J. Xu, "Quantitative Determination of the Probability of Multiple-Motor Transport in Bead-Based Assays," *Biophysical Journal* 110 (2016): 2720–2728, <https://doi.org/10.1016/j.bpj.2016.05.015>.
28. D. Hackney, "Kinesin ATPase: Rate-Limiting ADP Release," *Proceedings of the National Academy of Sciences of the United States of America* 85, no. 17 (1988): 6314–6318, <https://doi.org/10.1073/pnas.85.17.6314>.
29. T. Shimizu, E. Sablin, R. D. Vale, R. Fletterick, E. Pechatnikova, and E. W. Taylor, "Expression, Purification, ATPase Properties, and Microtubule-Binding Properties of the Ncd Motor Domain," *American Chemistry Society* 34, no. 40 (1995): 13259–13266, <https://doi.org/10.1021/bi00040a042>.
30. W. R. Schief, R. H. Clark, and A. H. Crevenna, "Inhibition of Kinesin Motility by ADP and Phosphate Supports a Hand-Over-Hand Mechanism," *Proceedings of the National Academy of Sciences* 101, no. 5 (2004): 1183–1188, <https://doi.org/10.1073/pnas.0304369101>.
31. R. A. Cross, "The Kinetic Mechanism of Kinesin," *Trends in Biochemical Sciences* 29, no. 6 (2004): 301–309, <https://doi.org/10.1016/j.tibs.2004.04.010>.
32. M. L. Kutys, J. Fricks, and W. O. Hancock, "Monte Carlo Analysis of Neck Linker Extension in Kinesin Molecular Motors," *Public Library of Science Computational Biology* 6, no. 11 (2010): e1000980, <https://doi.org/10.1371/journal.pcbi.1000980>.
33. A. Toleikis, N. J. Carter, and R. A. Cross, "Backstepping Mechanism of Kinesin-1," *Biophysical Journal* 119, no. 10 (2020): 1984–1994, <https://doi.org/10.1016/j.bpj.2020.09.034>.
34. J. Kerssemakers, J. Howard, H. Hess, and S. Diez, "The Distance That Kinesin-1 Holds Its Cargo From the Microtubule Surface Measured by Fluorescence Interference Contrast Microscopy," *Proceedings of the National Academy of Sciences* 103, no. 43 (2006): 15812–15817, <https://doi.org/10.1073/pnas.0510400103>.
35. M. V. Sataric, D. L. Sekulic, S. Zdravkovic, and N. M. Ralevic, "A Biophysical Model of How α -Tubulin Carboxy-Terminal Tails Tune Kinesin-1 Processivity Along Microtubule," *Journal of Theoretical Biology* 420 (2017): 152–157, <https://doi.org/10.1016/j.jtbi.2017.03.012>.

36. A. Marx, J. Müller, E.-M. Mandelkow, A. Hoenger, and E. Mandelkow, "Interaction of Kinesin Motors, Microtubules, and Maps," *Journal of Muscle Research & Cell Motility* 27, no. 2 (2006): 125–137, <https://doi.org/10.1007/s10974-005-9051-4>.
37. Z. Zhang, Y. Goldtzvik, and D. Thirumalai, "Parsing the Roles of Neck-Linker Docking and Tethered Head Diffusion in the Stepping Dynamics of Kinesin," *Proceedings of the National Academy of Sciences* 114 (2017): E9838–E9845, <https://doi.org/10.1073/pnas.1706014114>.
38. E. C. Thomas and J. K. Moore, "Selective Regulation of Kinesin-5 Function by β -Tubulin Carboxy-Terminal Tails," *Journal of Cell Biology* 224, no. 3 (2025): e202405115, <https://doi.org/10.1083/jcb.202405115>.
39. Y. Liu and Z. Zhang, "Origin of Tradeoff Between Movement Velocity and Attachment Duration of Kinesin Motor on a Microtubule," *Chinese Physics B* 33, no. 2 (2024): 028708, <https://doi.org/10.1088/1674-1056/ad1177>.
40. K. S. Thorn, J. A. Ubersax, and R. D. Vale, "Engineering the Processive Run Length of the Kinesin Motor," *Journal of Cell Biology* 151 (2000): 1093–1100, <https://doi.org/10.1083/jcb.151.5.1093>.
41. F. Mitra Shojania, B. R. Janakaloti Narayanareddy, O. Vadpey, et al., "Microtubule C-Terminal Tails Can Change Characteristics of Motor Force Production," *Traffic* 16, no. 10 (2015): 1075–1087, <https://doi.org/10.1111/tra.12307>.
42. C. Tucker and L. S. B. Goldstein, "Probing the Kinesin-Microtubule Interaction," *Journal of Biological Chemistry* 272, no. 14 (1997): 9481–9488, <https://doi.org/10.1074/jbc.272.14.9481>.
43. M. Bovyn, B. R. J. Narayanareddy, S. Gross, and J. Allard, "Diffusion of Kinesin Motors on Cargo Can Enhance Binding and Run Lengths During Intracellular Transport," *Molecular Biology of the Cell* 32, no. 9 (2021): 984–994, <https://doi.org/10.1091/mbc.e20-10-0658>.
44. T. Nguyen, B. R. J. Narayanareddy, S. P. Gross, and C. E. Miles, "Competition Between Physical Search and a Weak-to-Strong Transition Rate-Limits Kinesin Binding Times," *PLoS Computational Biology* 20, no. 5 (2024): e1012158, <https://doi.org/10.1371/journal.pcbi.1012158>.
45. M. Andreu-Carbó, C. Egoldt, M.-C. Velluz, and C. Aumeier, "Microtubule Damage Shapes the Acetylation Gradient," *Nature Communications* 15, no. 1 (2024): 2029, <https://doi.org/10.1038/s41467-024-46379-5>.
46. K. P. Wall, H. Hart, T. Lee, C. Page, T. L. Hawkins, and L. E. Hough, "C-Terminal Tail Polyglycylation and Polyglutamylolation Alter Microtubule Mechanical Properties," *Biophysical Journal* 119 (2020): 2219–2230, <https://doi.org/10.1016/j.bpj.2020.09.040>.
47. H. Jans, X. Liu, L. Austin, G. Maes, and Q. Huo, "Dynamic Light Scattering as a Powerful Tool for Gold Nanoparticle Bioconjugation and Biomolecular Binding Studies," *Analytical Chemistry* 81 (2009): 9425–9432, <https://doi.org/10.1021/ac901822w>.
48. S. A. Sisson, Y. Fan, and M. M. Tanaka, "Sequential Monte Carlo Without Likelihoods," *Proceedings of the National Academy of Sciences* 104, no. 6 (2007): 1760–1765, <https://doi.org/10.1073/pnas.0607208104>.

Supporting Information

Additional supporting information can be found online in the Supporting Information section.